

## Forced Convection over a Cylindrical Heating Element: Air Flow along the Surface of a Solid Cylinder

Isaac Ball\*  
Hanover College  
balli22@hanover.edu

### ABSTRACT

*In an attempt to confirm a correlation between the Nusselt number and the Graetz number for heat transfer over a cylinder's surface, a convection heat transfer experiment was conducted in which a ball valve attached to an air compressor was used to vary the air velocity through a rectangular pipe. A cylindrical heating element was placed within the pipe and was oriented with its axis parallel to the air flow through the pipe. PID's (Proportional Integral Derivative controllers) were used to measure the pipe's inlet and outlet temperature and the surface temperature of the heating element. After the air exited the rectangular pipe, it passed through a cylindrical pipe with a pitot tube. The pitot tube was connected to a hose which acted as a U-tube manometer. This manometer measured the difference in the air flow's stagnation pressure with the atmospheric air pressure through the pipe. The air then exited the pipe into the atmosphere. For each valve angle, the inlet temperature of the pipe, surface temperature of the heating element, outlet temperature of the pipe, and water level height difference within the manometer were recorded. Increasing the air velocity resulted in an increasing mass flow rate, which in turn increased the Reynolds number of the air flow. Increasing the mass flow rate also resulted in increasing heat transferred to the air. All Reynold's numbers found in this experiment were either laminar or barely in the transition phase. This would imply that the Nusselt number would remain constant throughout the experiment. However, this was not the case given the recorded data. The Nusselt numbers increased with*

*increasing air flow. This is most likely a result of the air flow not being fully developed in the heated section as suggested by the calculated Graetz number.*

Keywords:

Air Velocity  
Mass Flow Rate  
Stagnation Pressure  
Atmospheric Pressure  
Heat Transfer  
Reynold's Number  
Nusselt Number  
Graetz Number

### Nomenclature

$A_{cyl}$	Internal Cross-Sectional Area of the Cylindrical Pipe Segment
$A_{HE}$	Cross-Sectional Area of the Cylindrical Heating Element
$A_s$	Surface Area of the Heating Element
$A_{squ}$	Internal Cross-Sectional Area of the Rectangular Pipe Segment
$c_p$	Specific Heat Capacity of Air at Constant Pressure (1 atm)
$d_1$	Inner Diameter of Cylindrical Pipe (17 mm) [3]
$d_2$	Outer Diameter of Pitot Tube (3 mm) [3]
$D_h$	Hydraulic Diameter of the Rectangular Pipe Section
$D_{HE}$	Diameter of the Heating Element (6.60mm)
$g$	Gravitational Constant (9.81 m/s <sup>2</sup> )

$Gz_{Dh}$	Graetz Number Based on Hydraulic Diameter of the Rectangular Pipe Section	$Re_{Dh}$	Reynolds Number Based on Hydraulic Diameter of Rectangular Pipe Section
$h$	Water Height Difference within the Manometer	$T_1$	Inlet Air Temperature
$\bar{h}$	Average Convective Heat Transfer Coefficient of Air Flowing over the Cylinder	$T_2$	Heating Element Surface Temperature
$k$	Thermal Conductivity of Air	$T_3$	Outlet Air Temperature
$L$	Length of the Heating Element (460mm)	$T_b$	Average Bulk Temperature of the Air
$l$	Horizontal Dimension of Rectangular Cross-Sectional Area (70mm)	$u_{cyl}$	Air Velocity through the Cylindrical Pipe
$\dot{m}$	Mass Flow Rate	$u_{squ}$	Air Velocity through the Rectangular Pipe
$\overline{Nu}_D$	Average Nusselt Number over the Cylindrical Heating Element	$V$	Valve Angle
$\overline{Nu}_{Di}$	Average Nusselt Number over the Cylindrical Heating Element (Laminar Flow Correlation [4])	$w$	Vertical Dimension of Rectangular Cross-Sectional Area (45mm)
$\overline{Nu}_{Dt}$	Average Nusselt Number over the Cylindrical Heating Element (Turbulent Flow Correlation [4])	$x_{EL}$	Thermal Entry Length
$\overline{Nu}_{DP}$	Average Nusselt Number over the Cylindrical Heating Element as Predicted by the Turbulent and Laminar Correlations [4]	$\gamma_{H2O}$	Specific Weight of Water at Standard Conditions (9800 N/m <sup>3</sup> ) [2]
$\overline{Nu}_{th}$	Theoretical Nusselt Number as Predicted by the Correlations seen in Lienhard and Lienhard [1]	$\nu$	Kinematic Viscosity
$P_{HE}$	Perimeter of the Cylindrical Heating Element	$\rho_{air1}$	Density of Air at Pipe Inlet
$PID$	Proportional Integral Derivative Controller	$\rho_{air3}$	Density of Air at Pipe Outlet
$Pr$	Prandtl Number for Air		
$P_{squ}$	Perimeter of the Rectangular Cross-Sectional Area		
$P_{st}$	Static Pressure within Pitot Tube		
$P_{stag}$	Stagnation Pressure within Pitot Tube		
$Q$	Heat Transfer from the Heating Element		

## 1. INTRODUCTION

The Nusselt number is a critical heat transfer variable that depends largely on the specific situation in which it is employed. The Nusselt number allows one to find the convective heat transfer coefficient and, as seen in this experiment, determine the heat transfer from the heating element to the air.

There is no Nusselt number equation listed in *A Heat Transfer Textbook Fifth Edition* by Lienhard and Lienhard [1] for forced convection for a fluid flowing axially along the surface of a cylindrical heating element. Therefore, this experiment was performed in order to determine how the Nusselt number behaves for this specific situation.

The parameters measured during this experiment were  $T_1$ ,  $T_2$ ,  $T_3$ ,  $h$ ,  $l$ ,  $w$ ,  $L$ , and  $D_{HE}$ . First, it is necessary to determine the air velocity through the rectangular

section of the pipe. This is found via the continuity equation below [2].

$$\dot{m} = \rho_{air1} A_{squ} u_{squ} = \rho_{air3} A_{cyl} u_{cyl} \quad (1)$$

This implies the following equation:

$$u_{squ} = \frac{\rho_{air3} A_{cyl}}{\rho_{air1} A_{squ}} u_{cyl} \quad (2)$$

where the areas are defined below in Eq. 3 and Eq. 4. A detailed schematic of the pitot tube area may be seen below in Figure 1.

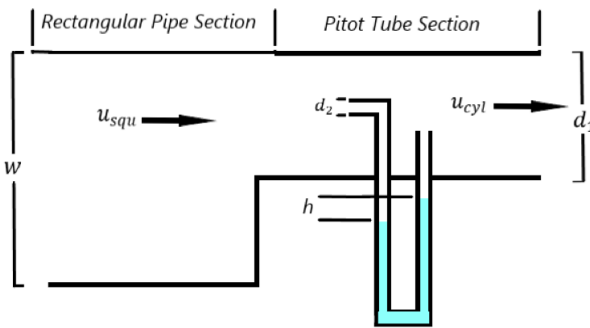


Figure 1: Pitot Tube Detail

$$A_{cyl} = \frac{(d_1^2 - d_2^2) * \pi}{4} = 2.2 * 10^{-4} m^2 \quad (3)$$

$$A_{squ} = l * w = 0.0032 m^2 \quad (4)$$

Note that Eq. 4 neglects the cross-sectional area of the heating element since the heating element's diameter was relatively small (6.60mm) when compared to the rectangular pipe's cross-sectional area. The height difference within the manometer may be converted to the velocity within the cylinder via Bernoulli's Equation [2]. Note that the Bernoulli Equation is applied across the pitot tube.

$$P_{stag} = P_{st} + \frac{1}{2} \rho_{air3} u_{cyl}^2 = P_{st} + \gamma_{H2O} h \quad (5)$$

This allows the velocity through the cylinder to be expressed as follows:

$$u_{cyl} = \sqrt{\frac{2\gamma_{H2O} h}{\rho_{air3}}} \quad (6)$$

Therefore, the velocity through the square section of the pipe may be found with the following equation:

$$u_{squ} = \frac{\rho_{air3} A_{cyl}}{\rho_{air1} A_{squ}} \sqrt{\frac{2\gamma_{H2O} h}{\rho_{air3}}} \quad (7)$$

All air properties aside from the densities at the pipe's inlet and outlet ( $\rho_{air1}$  and  $\rho_{air3}$  respectively) are evaluated at the average bulk temperature of the air as defined in Eq. 8.

$$T_b = \frac{T_1 + T_3}{2} \quad (8)$$

Once the air velocity through the rectangular pipe has been found, the heat transfer from the heating element to the air may be found with Eq. 9, assuming that the heat loss from the pipe is negligible. Note that Eq. 1 may be used to find the mass flow rate.

$$Q = \dot{m} c_p (T_3 - T_1) \quad (9)$$

For forced convection, the heat transfer may be found via Eq. 10.

$$Q = A_s \bar{h} (T_2 - T_b) \quad (10)$$

Note that Eq. 10 uses the average bulk temperature of the air. Therefore, evaluating Eq. 10 will yield the average heat transfer from the heating element. The surface area of the heating element is defined as follows:

$$A_s = \pi D_{HE} L + \frac{1}{2} \pi D_{HE}^2 \quad (11)$$

Therefore, the average convective heat transfer coefficient can be calculated as follows:

$$\bar{h} = \frac{\dot{m} c_p (T_3 - T_1)}{A_s (T_2 - T_b)} \quad (12)$$

Once the average convective heat transfer coefficient has been found, the Nusselt number may be found via Eq. 13:

$$\overline{Nu_D} = \frac{hD_h}{k} \quad (13)$$

where the hydraulic diameter is defined in Eq. 14.

$$D_h = \frac{4(A_{sq} - A_{HE})}{P_{sq} + P_{HE}} = \frac{4(A_{sq} - \pi(\frac{D_{HE}}{2})^2)}{(2l + 2w + \pi D_{HE})} \quad (14)$$

It should be noted that the Reynolds number for this scenario may be found via Eq. 15 [1].

$$Re_{Dh} = \frac{u_{sq} D_h}{\nu} \quad (15)$$

According to Lienhard and Lienhard [1], the Reynolds number calculated from the hydraulic diameter of a non-circular duct may be used to determine whether a fluid flow is laminar or turbulent. It is assumed that the flow transitions to turbulent when the Reynolds number exceeds 2300 [1]. The two equations below may be used to determine the Graetz number and the thermal entry length for this scenario [1].

$$\frac{x_{EL}}{D_h} = 0.034 Re_{Dh} Pr \quad (16)$$

$$Gz_{Dh} = \frac{Re_{Dh} Pr D_h}{L} \quad (17)$$

Note that Eq. 16 assumes that the wall temperature within the pipe remains constant. This equation may be used since the temperature of the heating element surface remains constant and the inlet and outlet temperatures of the fluid do not largely vary (see Table 2).

## 2. MATERIALS AND METHODS

### 2.1 Experimental Setup

See Figures 2-7 for detailed views of the experimental setup. A generic mini ball valve with a quarter inch inner diameter was used with a DeWalt D55168 Oil Free Portable Air Compressor. The rectangular pipe section (interior dimensions: 70mm x 45mm x

460mm) was made of steel. The valve was connected to the rectangular pipe via EZ-FLOW Clear Vinyl Tubing with an inner diameter of 15mm and Scotch Electrical Tape. The outlet of the rectangular pipe was connected to the GUNT HM 150.13 Pitot Tube via electrical tape. Three REX-C100 PID controllers, three Type K Thermocouples, 14 AWG Remington Wire, a WERLAHO SSR-40DA relay, and a VEVOR Variac TDGC-1KM Transformer were used to control and measure the temperatures throughout the system. They are connected as seen in Figure 7. A heating element from a George Foreman Lean Mean Fat Reducing Grilling Machine was used to heat the air in this lab. Note that a STAEDTLER protractor was used to measure the angle of the valve handle, and a SWANSON yardstick was used to measure the height difference of water within the manometer.

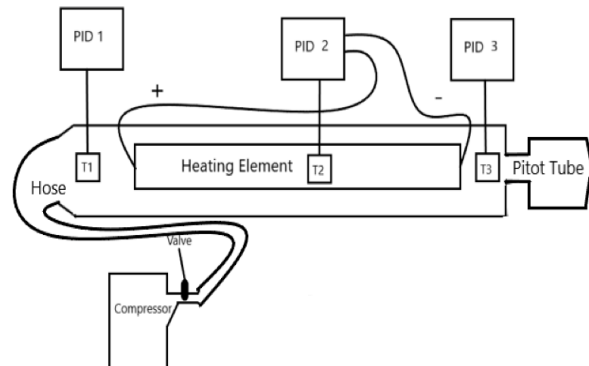


Figure 2: Experimental Schematic

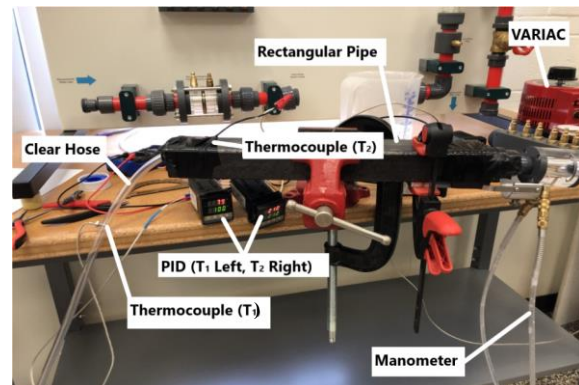


Figure 3: Experimental Setup Part 1

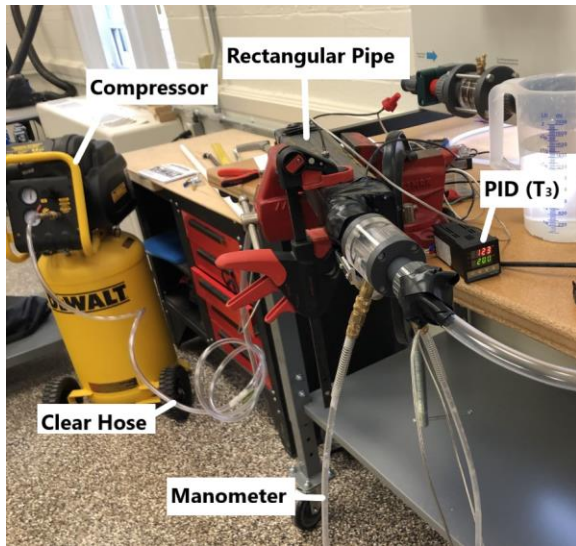


Figure 4: Experimental Setup Part 2

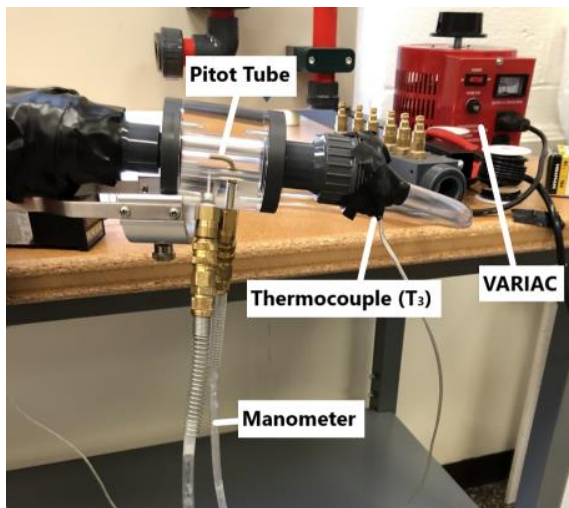


Figure 5: Pitot Tube Detail

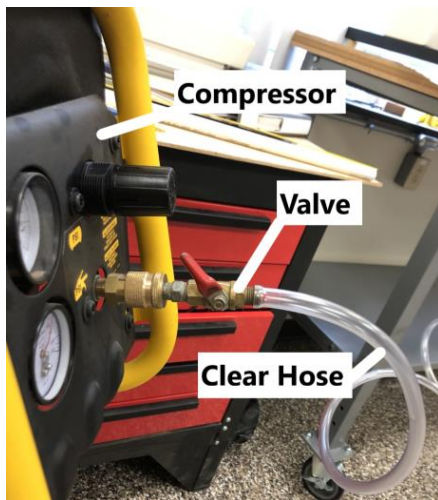


Figure 6: Compressor Detail

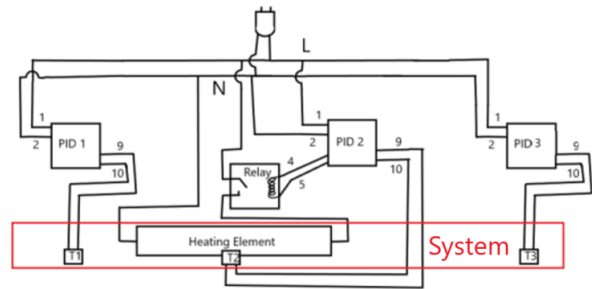


Figure 7: Circuit Schematic

## 2.2 Experimental Procedure

First, the experimental system was assembled as seen in Figures 2-7. The valve handle was set to  $40^\circ$  from the axis of the valve. The VARIAC was set to 120V, and the second PID (which measures and controls  $T_2$ ) was set to  $212^\circ\text{F}$ . The PID's were allowed to stabilize with  $T_2$  reaching  $212^\circ\text{F}$ . The height difference in the manometer and  $T_1$  and  $T_3$  were then recorded. This process was repeated for valve handle angles of  $30^\circ$ ,  $20^\circ$ ,  $10^\circ$ , and  $0^\circ$  from the axis of the valve. The recorded data may be seen below in Table 1.

Table 1: Recorded Data

$V$ ( $^\circ$ )	$T_1$ ( $^\circ\text{F}$ )	$T_2$ ( $^\circ\text{F}$ )	$T_3$ ( $^\circ\text{F}$ )	$\Delta h$ (mm)
40	84	212	181	5
30	103	212	203	6
20	112	212	200	8
10	114	212	202	11
0	112	212	200	12

## 3. RESULTS AND DISCUSSION

First, the temperatures listed in Table 1 were converted to absolute temperatures (see Table 2), and the average bulk temperature was found according to Eq. 8.

Table 2: Absolute Temperatures and Film Temperature

$V$ ( $^\circ$ )	$T_1$ (K)	$T_2$ (K)	$T_3$ (K)	$T_b$ (K)
40	302	373	356	329
30	312	373	368	340
20	317	373	366	342
10	319	373	367	343
0	317	373	366	342

Next the inlet and outlet temperatures with Table A.6 from Lienhard and Lienhard [1] were used to find the densities at both the inlet and outlet of the system (see Table 3).

Table 3: Inlet and Outlet Densities

$V$ (°)	$T_1$ (K)	$T_3$ (K)	$\rho_{air1}$ (kg/m <sup>3</sup> )	$\rho_{air3}$ (kg/m <sup>3</sup> )
40	302	356	1.169	0.994
30	312	368	1.132	0.963
20	317	366	1.114	0.968
10	319	367	1.107	0.966
0	317	366	1.114	0.968

The average bulk temperatures and Table A.6 from Lienhard and Lienhard [1] were then used to determine the thermal conductivity, specific heat capacity for constant pressure, kinematic viscosity, and Prandtl number for the air at each average bulk temperature (see Table 4).

Table 4: Air Properties

$T_b$ (K)	$c_p$ (J/kg*K)	$k$ (W/m*K)	$\nu$ (m <sup>2</sup> /s)	$Pr$
329	1008	0.0285	1.855E-05	0.704
340	1009	0.0293	1.966E-05	0.703
342	1009	0.0294	1.987E-05	0.703
343	1009	0.0295	1.997E-05	0.703
342	1009	0.0294	1.987E-05	0.703

It should be noted that for temperatures not explicitly listed on Table A.6 [1], a linear relationship was assumed between each of the adjacent table points. The constants were then found via linear interpolation between the two adjacent points. It was then possible to find both the air velocity through the rectangular pipe and the air mass flow rate via Eq. 7 and Eq. 1 respectively (see Table 5)

Table 5: Rectangular Pipe Velocity and Mass Flow Rate

$V$ (°)	$\Delta h$ (mm)	$u_{squ}$ (m/s)	$\dot{m}$ (kg/s)
40	5	0.59	0.0022
30	6	0.66	0.0023
20	8	0.77	0.0027
10	11	0.91	0.0032
0	12	0.95	0.0033

Note here that the results are as expected. As the angle decreases, the valve opens, and more air is sent through the system. The mass flow rates are then used with Eqs. 11 and 12 to find the air flows' average convective heat transfer coefficients (see Table 7). Eqs. 13 and 14 may then be used to calculate the average Nusselt number for each air flow rate (see Table 7). Table 7.2 in *Kaviany's Essentials of Heat Transfer* contains the Nusselt number correlation information seen in Table 6 for laminar, fully developed, forced flow through the type of system used in this experiment (Circular Annuli: Inner-Surface Convection [4]).

Table 6: Laminar, Fully Developed, Forced Flow  $\overline{Nu}_D$  Correlations [4]

$\frac{D_{HE}}{D_h}$	$\overline{Nu}_{Dl}$
0.05	17.81
0.1	11.91
0.2	8.499
0.4	6.583
0.6	5.912
0.8	5.580
1	5.385

A plot of these correlations may be seen below in Figure 8.

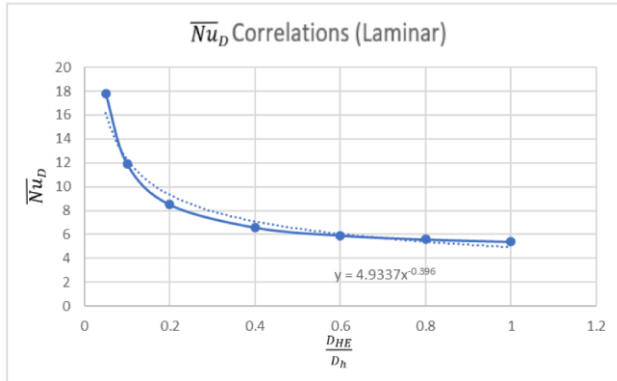


Figure 8:  $\overline{Nu}_D$  Correlations (Laminar)

As seen in Figure 8, the following equation closely approximates the correlations for laminar, fully developed, forced flow.

$$\overline{Nu}_{DI} = 4.9337 \left( \frac{D_{HE}}{D_h} \right)^{-0.396} \quad (18)$$

Since  $\frac{D_{HE}}{D_h} \approx 0.13$  for the conducted experiment, the average Nusselt number for laminar, fully developed, forced flow will be approximately 11 in the experimental scenario. For transitional flow (defined as  $2300 < Re_{Dh} < 10^4$ ), Kaviany suggests the following equation [4]:

$$\overline{Nu}_{DP} = \sqrt[10]{(\overline{Nu}_{DI})^{10} + \left( \frac{e^{\frac{2200 - Re_{Dh}}{365}}}{(Nu_{DI})^2} + \frac{1}{(Nu_{Dt})^2} \right)^{-5}} \quad (19)$$

Where  $\overline{Nu}_{DI}$  is given by Eq. 18 above and  $\overline{Nu}_{Dt}$  is given below in Eq. 20.

$$\overline{Nu}_{Dt} = 0.023 Re_{Dh}^{\frac{4}{5}} Pr^{0.4} \quad (20)$$

Note that Eq. 20 is only valid for  $0.7 < Pr < 160$ . Table 7 lists the average convective heat transfer coefficient, average Nusselt number based on the experimental measurements, the average Nusselt number as predicted by the turbulent or laminar correlations as appropriate (Eqs. 18-20), Graetz number, thermal entry length, and Reynolds number (calculated according to Eq. 15) for each valve angle.

Table 7:  $\bar{h}$ ,  $\overline{Nu}_D$ ,  $\overline{Nu}_{DP}$ ,  $Re_{Dh}$ ,  $x_{EL}$ , and  $Gz_{Dh}$  for Each Valve Angle

$V$ (°)	$\bar{h}$ (W/m <sup>2</sup> *K)	$\overline{Nu}_D$	$\overline{Nu}_{DP}$	$Re_{Dh}$	$x_{EL}$ (m)	$Gz_{Dh}$
40	280	487	11	1579	1.9	120
30	417	708	11	1659	2.0	126
20	450	760	11	1931	2.3	147
10	533	899	11	2265	2.7	172
0	551	931	11	2365	2.8	180

Note that the thermal entry length for each flow is longer than the heating element and rectangular pipe segment. Therefore, all flows analyzed in this lab are not fully developed. This could be the primary cause for the large error between the calculated experimental Nusselt numbers and the predicted Nusselt numbers. A mass flow rate vs. Nusselt number plot may be seen in Figure 9 below.

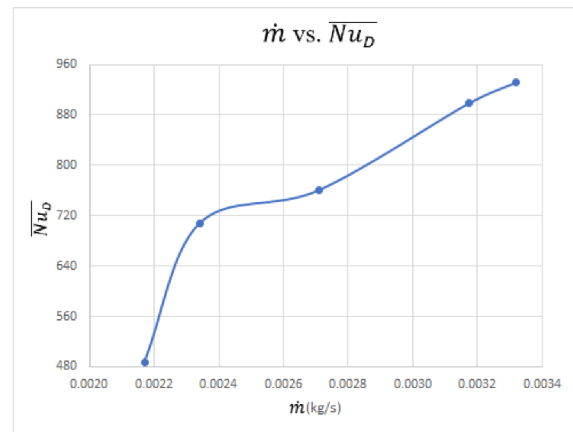


Figure 9:  $\dot{m}$  vs.  $\overline{Nu}_D$  Plot

Note that the slope between the first two points greatly differs from slope connecting the last three points. However, based on the Reynolds numbers seen in Table 6, the first four points are laminar, and the fifth point is just entering the transition flow regime. Since Nusselt number equations change based on whether the flow is laminar or turbulent [1], two different trend lines (one for laminar flow and one for turbulent flow) should be plotted to accompany the experimental data. However, there is only one point in the

turbulent flow regime, so it is impossible to plot a trend line for the turbulent flow regime without more data.

Lienhard and Lienhard provide the correlations seen in Figure 10 below for Nusselt number as a function of the Graetz number for a variety of scenarios.

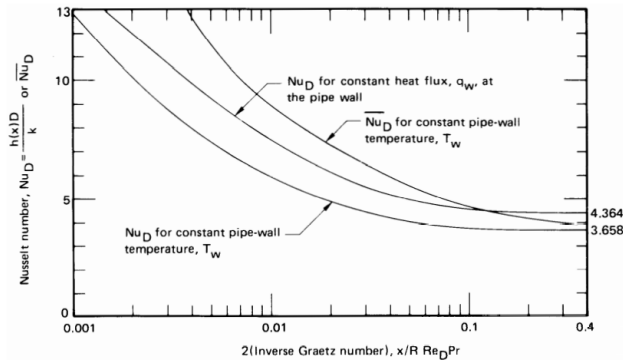


Figure 10:  $2Gz_{Dh}^{-1}$  vs.  $\overline{Nu}_D$  (Theoretical) [1]

According to the uppermost line in Figure 10 and given twice the inverse of the Graetz numbers seen in Table 7 (see Table 8), it would appear that the average Nusselt numbers for the scenario in question would result in Nusselt numbers ranging from approximately 7.5 to 9. A linear relationship is assumed between these two Nusselt numbers, and the resulting trendline may be seen in Figure 11 below. The calculated average Nusselt numbers from Table 7 are divided by 100 so that they are of the same order of magnitude as the theoretical Nusselt numbers. These divided Nusselt numbers are plotted with the theoretical trendline in Figure 10 as well.

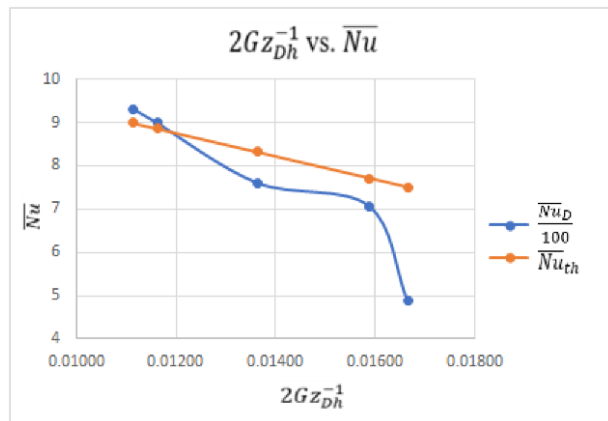


Figure 11:  $2Gz_{Dh}^{-1}$  vs.  $\overline{Nu}$

The values plotted in Figure 11 may be seen in Table 8 below.

Table 8:  $\frac{\overline{Nu}_D}{100}$ ,  $\overline{Nu}_{th}$ , and  $2Gz_{Dh}^{-1}$  for Each Valve Angle

$V$ ( $^\circ$ )	$2Gz_{Dh}^{-1}$	$\frac{\overline{Nu}_D}{100}$	$\overline{Nu}_{th}$
40	0.0166	4.87	7.5
30	0.0159	7.08	7.7
20	0.0136	7.60	8.3
10	0.0116	8.99	8.9
0	0.0111	9.31	9.0

Note that as twice the inverse of the Graetz number increases, the calculated average Nusselt number decreases as expected. However, the average Nusselt numbers seen in Table 7 are greater than the theoretical Nusselt numbers seen in Table 8 by a factor of 100.

#### 4. CONCLUSION

As seen in Figure 9, it is clear that as the mass flow rate increases, the Nusselt number increases as well. This result should be expected since  $\overline{Nu}_D \propto h \propto \dot{m}$  (see Eqs. 12 and 13). As the valve was opened, the air flow rate increased. This resulted in increasing Reynolds numbers and Nusselt numbers as expected. However, the calculated Nusselt numbers were larger than expected by a factor of 100. This could be due to the flow regime not being fully developed during the experiment. This problem could be corrected by using a heating element and pipe longer than the maximum thermal entry length shown in Table 7. In addition to this, there seems to be some additional error with the first data point ( $V = 40^\circ$ ). This could be due to the inlet temperature ( $T_1$ ) for that data point being much different from the other data points' inlet temperature (see Table 1). Future development of this lab would include extending both the length of the heating element and the pipe to allow the flow regime to be fully developed during the



experiment and gathering more data from both laminar and turbulent flow regimes.

In future experimentation, a circular metal tube with a smaller cross-sectional area than the rectangular pipe would simplify the calculations required for this experiment and increase the range over which this experiment could be tested. Since the area of the circular pipe would be less than the area of the rectangular pipe, larger air velocities over the heating element would be able to be measured since  $u_{squ} \propto \frac{1}{A_{squ}}$  (Eq. 7).

### ACKNOWLEDGEMENTS

All materials were generously provided by the \*\*\*\*\*. Advising throughout the experimental process was given by \*\*\*\*\*.

### REFERENCES

- [1] Lienhard IV, John H. and Lienhard V, John H. *A Heat Transfer Textbook 5<sup>th</sup> Edition*. Phlogiston Press, 2020
- [2] Munson, Okiishi, Huebsch, Rothmayer. *Fundamentals of Fluid Mechanics 7<sup>th</sup> Edition*. John Wiley & Sons, Inc. 2013
- [3] Mittasch, Peter and Schröder, Klaus. *Experiment Instructions HM 150.13 Methods of Flow Measurement*. G.U.N.T. Gerätebau. 2017
- [4] Kaviany, Massoud. *Essentials of Heat Transfer*. Cambridge University Press. 2011